D221 in Thymidylate Synthase Controls Conformation Change, and Thereby Opening of the Imidazolidine[†,‡]

Carleton R. Sage,[§,||] Melissa D. Michelitsch,[§] Thomas J. Stout,[||] Donna Biermann, Robert Nissen, Janet Finer-Moore,* and Robert M. Stroud*

Department of Biochemistry and Biophysics, University of California at San Francisco, San Francisco, California 94143-0448

Received May 6, 1998; Revised Manuscript Received August 4, 1998

ABSTRACT: In thymidylate synthase (TS), the invariant residue Asp-221 provides the only side chain that hydrogen bonds to the pterin ring of the cofactor, 5,10-methylene-5,6,7,8-tetrahydrofolate. All mutants of D221 except cysteine abolish activity. We have determined the crystal structures of two ternary complexes of the *Escherichia coli* mutant D221N. In a complex with dUMP and the antifolate 10-propargyl-5,8-dideazafolate (CB3717), dUMP is covalently bound to the active site cysteine, as usual. CB3717, which has no imidazolidine ring, is also bound in the usual productive orientation, but is less ordered than in wild-type complexes. The side chain of Asn-221 still hydrogen bonds to N3 of the quinazoline ring of CB3717, which must be in the enol form. In contrast, the structure of D221N with 5-fluoro-dUMP and 5,10-methylene-5,6,7,8-tetrahydrofolate shows the cofactor bound in two partially occupied, nonproductive binding sites. In both binding modes, the cofactor has a closed imidazolidine ring and adopts the solution conformation of the unbound cofactor. In one of the binding sites, the pterin ring is turned around such that Asn-221 hydrogen bonds to the unprotonated N1 instead of the protonated N3 of the cofactor. This orientation blocks the conformational change required for forming covalent ternary complexes. Taken together, the two crystal structures suggest that the hydrogen bond between the side chain of Asp-221 and N3 of the cofactor is most critical during the early steps of cofactor binding, where it enforces the correct orientation of the pterin ring. Proper orientation of the cofactor appears to be a prerequisite for opening the imidazolidine ring prior to formation of the covalent steady-state intermediate in catalysis.

Thymidylate synthase (TS)[1] methylates 2′-deoxyuridine 5′-monophosphate (dUMP) to produce thymidine 5′-monophosphate (dTMP), a nucleotide essential for synthesis of DNA. The cofactor 5,10-methylene-5,6,7,8-tetrahydrofolate (CH_2H_4folate) serves as both a methyl donor and reductant in the reaction (Figure 1). Amino acid residues lining the active site of TS are highly conserved across species, yet mutagenesis has shown that very few of the invariant residues are essential for the catalytic activity of the protein (*1*, *2*). The active site cysteine, Cys-198(146),[2] activates the C5 position of dUMP for condensation with a methyl group of the cofactor, and is an essential residue (*3*). Mutations of a second critical residue, Glu-60, reduce k_{cat}/K_m by factors of 10^3-10^5, and this residue has been implicated in chemical steps following formation of intermediate II (*4*−*6*). Arg-218 is also essential for activity, mainly because of its role in maintaining the structure of the active site (unpublished). We now investigate the role of a fourth invariant active site residue, Asp-221(169), which is unusually sensitive to mutation. Of 19 Asp-221 mutants made in *Lactobacillus casei* TS, and 14 mutants made in *Escherichia coli* TS, only D221C can support growth of a thymidylate synthase-deficient host, indicating activity at above the ∼1% level (*2*, *7*). The abrogation of TS activity by mutation of D221 opened the possibility of isolating a reaction intermediate preceding the affected step which could be studied by crystallography, and prompted our structure studies.

Asp-221(169) presents the only side chain which hydrogen bonds to the pterin ring of CH_2H_4folate (*8*−*10*). Asp-221-(169) is proposed to play a critical role not only in binding the cofactor but also in stabilizing the closed conformation of the enzyme seen in crystal structures of ternary complexes

[†] This research was supported by NIH Grant RO1-CA41323 to J.F.-M.

[‡] Coordinates for the structures of the D169N complexes with dUMP and CB3717 and with FdUMP and CH_2H_4folate are deposited in the PDB with accession codes 1dna and 1bjg, respectively.

* To whom correspondence should be addressed.

[§] The first two authors contributed equally to this work.

[||] Current address: *Meta*Xen, LLC, 3910 Trust Way, Hayward, CA 94545.

[1] Abbreviations: TS, thymidylate synthase; dUMP, 2′-deoxyuridine 5′-monophosphate; CH_2H_4folate, 5,10-methylene-5,6,7,8-tetrahydrofolate; THF, 5,10-methylene-5,6,7,8-tetrahydrofolate; dTMP, thymidine 5′-monophosphate; 5-bromo-dUMP, 5-bromo-2′-deoxyuridine 5′-monophosphate; CB3717, 10-propargyl-5,8-dideazafolate; F_o, measured structure factor amplitude; F_c, calculated structure factor amplitude; $(2F_o - F_c)\alpha_{calc}$ map, electron density map calculated with coefficients $2F_o - F_c$ and phases derived from the coordinates of the structure; $(F_o - F_c)\alpha_{calc}$ map, electron density map calculated with coefficients $F_o - F_c$ and phases derived from the coordinates of the structure; D221-(169)N, mutant in which aspartate-221 is substituted by asparagine.

[2] The numbering scheme is that of *L. casei* TS, with *E. coli* numbering based on sequence alignment in parentheses. To convert from *L. casei* to *E. coli* numbering, subtract 2 for numbers ≤89 and subtract 52 for numbers >89.

S0006-2960(98)01051-4 CCC: $15.00
Published on Web 09/05/1998

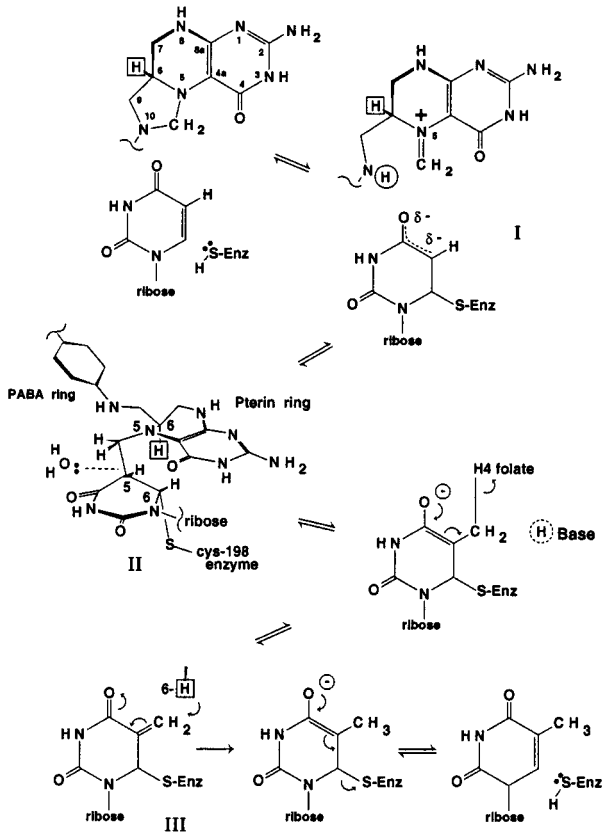

FIGURE 1: Major chemical steps in the TS mechanism.

(*8*, *11*). The most dramatic differences between the open and closed conformations are the ordering and movement of the C terminus and Arg-23(21) into the active site. These, and other, less dramatic shifts in protein segments promote catalysis by closing off the active site cavity to bulk solvent and reducing the mobility of the ligands. The carboxyl group of Asp-221 is part of a hydrogen bond network, involving two conserved waters, which tethers the C terminus and Arg-23(21) to the cofactor in the closed conformation of the enzyme.

The importance of Asp-221 for cofactor binding is underscored by the fact that only four of the seven highly characterized *L. casei* TS mutants form detectable amounts of the ternary complex with CH_2H_4folate and the inhibitor 5-fluoro-dUMP (FdUMP) (*7*). The ability of a TS mutant to form the FdUMP ternary complex is an indication of whether it can progress to intermediate II (Figure 1) in the enzyme reaction. The apparent K_d for covalent complex formation with CH_2H_4folate, that is, the product of the equilibrium constants for noncovalent binding and covalent complex formation, is estimated to be at least 10^6-fold higher than that of wild-type TS for three of the four *L. casei* TS mutants (D221S, D221E, and D221A) which form detectable amounts of the FdUMP ternary complex. Only D221C binds CH_2H_4folate stoichiometrically with an apparent K_d of <1 μM. One of the seven well-characterized *L. casei* TS mutants that drastically affects the rate of covalent complex formation with the cofactor and FdUMP, reducing it to unmeasurably small values, is D221(169)N. dUMP binding, however, is relatively unimpaired; K_d^{dUMP} for D221(169)N is only ~20-fold higher than that for wild-type TS (*7*). This raises the question as to which chemical or structural mechanism depends on the crucial D221(169). We report here the structural basis for the profound effects on cofactor binding of this conservative substitution, D169N in *E. coli*.

MATERIALS AND METHODS

Preparation of the Protein, Crystallization, and Data Collection. An aspartic acid to asparagine point mutation at position 169 of *E. coli* TS was made by the method of Kunkel et al. (*12*) in the ThyA gene (*13*) which had been cloned into the Bluescript vector (Stratagene). Positive clones were identified by DNA sequence analysis. Mutant *E. coli* TS was expressed in *E. coli* χ2913 (thy−) (*14*), which lacks a gene for TS, and purified as described by Maley and Maley (*15*). The activity of the mutant was assayed by monitoring the change in absorbance at 340 nm, which accompanies the formation of dihydrofolate (*16*). The ability of the mutant to form the covalent ternary complex (intermediate II, Figure 1) was assayed by SDS−PAGE of D221(169)N−FdUMP−CH_2H_4folate complexes, as described previously (*7*). The enzyme−FdUMP−CH_2H_4folate complex is a close intermediate of intermediate II.

For crystallization, the purified protein was dialyzed against 20 mM KPO_4 (pH 7.5), 0.1 mM EDTA, and 10 mM BME. Crystals were grown by vapor diffusion at room temperature and pH 7.6−7.8 from a solution that contained ~15 mg/mL protein, 20 mM potassium phosphate, 2.3 M ammonium sulfate, 100 mM $MgCl_2$, and either 20 mM dUMP and 4.8 mM CB3717 or 20 mM FdUMP and 10 mM CH_2H_4folate. Crystals of D169N TS−dUMP−CB3717 grew as hexagonal rods, the normal form for ternary complexes. For crystallization of D169N TS−FdUMP−CH_2H_4folate, wells were purged with argon and crystals were grown in the dark; cubic crystals, the normal form for crystals of the apoprotein, appeared in 1−2 days.

X-ray diffraction data were collected at room temperature on an RAXIS-IIc imaging plate system using monochromatized CuKα radiation, from a Rigaku rotating anode generator operating at 50 kV and 300 mA. We have identified cryoprotectant solutions which allow us to freeze *E. coli* TS ternary complex crystals; however, we found that measuring the data at −170 °C does not extend its resolution beyond that of room-temperature data. The crystals did not decay significantly during the period when data were collected. Data were reduced to I_{hkl}'s using Denzo/Scalepack (*17*).

Structure Solution and Refinement. The mutant complexes were isomorphous to previously determined crystal forms of liganded, and of apo wild-type *E. coli* TS. Structure solution was based on the difference Fourier technique (*18*). In the case of D169N TS−dUMP−CB3717, an initial rigid-body refinement using the wild-type ternary complex structure, without substrate or waters, was carried out in X-PLOR (*19*). This was followed by fitting of the substrate into $(F_o - F_c)\alpha_{calc}$ maps using the program CHAIN, alternating rounds of side chain rebuilding with simulated annealing (*20*) and energy minimization. Individual atomic *B*-factors were refined and water molecules included. The structures of the wild-type and D169N ternary complexes with dUMP and CB3717 were compared using direct difference maps, calculated with coefficients $(F_{o1} - F_{o2})\alpha_{calc}$.

The D169N TS−FdUMP−CH_2H_4folate structure was solved by molecular replacement using the CCP4 version

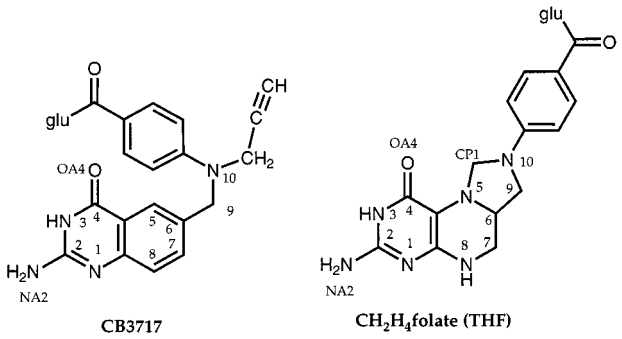

FIGURE 2: Chemical structures for the antifolate CB3717 and the TS cofactor, CH_2H_4folate.

of AMORE. The wild-type *E. coli* TS−dUMP structure (*21*), with dUMP and waters removed, was employed as the search probe. Water molecules were fitted to the density, and dummy waters were placed in the density for the ligands. After rigid-body refinement of this initial solution, with waters added, FdUMP and CH_2H_4folate were fitted into a $(3F_o - 2F_c)\alpha_{calc}$ map. After several alternating rounds of positional and *B*-factor refinement carried out using X-PLOR, and manual rebuilding, waters were revised and a second site for the cofactor was identified in difference maps. The two alternate positions for cofactor were initially refined at half-occupancy. As a final step, the occupancies of the two cofactor sites and dUMP were refined without constraints.

RESULTS

The D221(169)N mutation in *E. coli* TS was engineered and the protein purified, and two ternary complexes with substrates and inhibitors, D221(169)N TS−dUMP−CB3717 and D221(169)N TS−FdUMP−CH_2H_4folate, were crystallized and analyzed by X-ray diffraction. In wild-type TS, both of these complexes are analogues of a key reaction intermediate (II) in dUMP methylation (Figure 1) (*4*, *9*, *22*). The first complex contains the natural substrate, dUMP, and a cofactor analogue, CB3717, which functions as a competitive inhibitor (*23*). CB3717 differs from CH_2H_4folate by having a quinazoline instead of a pterin ring, and by not having a five-membered, imidazolidine ring (Figure 2); thus, it resembles the activated form of the cofactor in which the imidazolidine ring has opened to give an iminium ion at CP1. In the activated cofactor, the iminium ion CP1 is attached to N5 of CH_2H_4folate and attacks C5 of dUMP (Figure 1), whereas in CB3717, CP1 is absent, N10 is derivatized with a propargyl group, and the inhibitor does not form a covalent link to dUMP. However, in the wild-type complex, the catalytic cysteine bonds to C6 of dUMP to generate an analogue of covalent intermediate II with no bond possible between dUMP and CB3717.

The second complex contains the natural cofactor, CH_2H_4-folate, and a substrate analogue, 5-fluoro-dUMP (FdUMP) which differs from dUMP only by substitution of the hydrogen at C5 with fluorine. In wild-type TS, the crystal structure of this complex shows that the cofactor imidazolidine ring has opened and the resulting iminium ion has added to C5 of FdUMP to give a close analogue of intermediate II (Figure 1) (*10*, *24*). We have determined and refined the crystal structures of the two D221N ternary complexes to 2.2 and 2.3 Å resolution, respectively (Table 1).

Table 1: Crystallographic Statistics

statistic	CH_2H_4folate complex	CB3717 complex	
space group	$I2_13$	$P6_3$	
asymmetric unit	one protomer	one dimer	
unit cell [*a*, *b*, *c* (Å)]	133.0, 133.0, 133.0	127.2, 127.2, 68.2	
resolution (Å)	2.3	2.2	
R_{merge} (%)[a] (final shell)	7.5 (25.1)	5.9 (18.4)[c]	
completeness (%)	94.9 (90.1)	78.4 (52.6)[c]	
no. of observations	68 196	37 087[c]	
no. of reflections in refinement	16 234	24 287	
R_{cryst} (%)[b]	16.9	18.0	
R_{free} (%)	22.9	22.6	
$rmsd_{bondlengths}$ (Å)	0.010	0.005	
$rmsd_{angles}$ (deg)	1.6	1.5	
$rmsd_{dihedrals}$ (deg)	25.1	24.9	
$rmsd_{impropers}$ (deg)	1.3	1.1	
no. of waters	92	216	
B-factor or occupancy		monomer 1	monomer 2
$\langle B\rangle_{protein}$ (Å^2)	25	23	30
$\langle B\rangle_{dUMP}$ (Å^2)	51	32	48
$\langle B\rangle_{THF(CB3717)}$ (Å^2)	54 and 53	46	64
$occupancy_{dUMP}$ (%)	58	100	100
$occupancy_{THF(CB3717)}$	35 and 43	100	100

[a] $R_{merge} = \sum|I - \langle I\rangle|/\sum|\langle I\rangle|$; negative intensities included as zero. [b] $R_{cryst} = \sum||F_o| - |F_c||/\sum|F_o|$. [c] Statistic for data with $I > 1\sigma(I)$.

The D221(169)N Complex with dUMP and CB3717 Supports Productive Binding of the Substrate and Cofactor Analogue. Given the drastic effects of the D221(169)N mutation on K_d^{THF} (*7*), it is surprising that in the crystal structure of D221(169)N TS−dUMP−CB3717, dUMP and CB3717 are aligned in the active site in a manner almost identical to that seen in the wild-type enzyme, with dUMP covalently bound to the catalytic cysteine, Cys-198(146) (*6*, *8*) (Figure 3). The direct difference map between the wild-type and the D221(169)N complexes indicates a shift of the cofactor by less than 0.5 ± 0.2 Å away from Asn-221(169) (Figure 4). It is also apparent from both the direct difference map and the refined *B*-factors of the ligands that both dUMP and CB3717 are less ordered in D221(169)N than in wild-type TS (Table 1). The average *B*-factors for the atoms in CB3717 in both crystallographically independent protomers of the dimeric enzyme were approximately 2 times greater than the average *B*-factor for the protein atoms in the respective protomer. The average *B*-factors for the atoms of dUMP were approximately 1.5 times greater than the average *B*-factors for the protein. In the wild-type complex, the ratios of ligand *B*-factors to protein *B*-factors were 1.3 and 0.8 for CB3717 and dUMP, respectively (*6*).

The orientation of the carboxamide group of Asn-221-(169) cannot be determined directly from the electron density, but can be deduced from changes in hydrogen bonding (Figure 5), which are seen in both active sites in the crystal structure. In wild-type TS−dUMP−CB3717, Wat3 is a hydrogen bond acceptor from NA2 of CB3717 and the amide group of Ala-315(263), and a hydrogen bond donor to the carboxyl of Asp-221 and another water molecule. In the mutant structure, Wat3 is 3.5 Å from NA2 of CB3717, indicating that Wat3 no longer accepts a hydrogen bond from the cofactor. We surmise that Wat3 instead accepts a hydrogen bond from Nδ2 of the Asn-221(169) carboxamide group, as well as from the amide of Ala-315(263). The

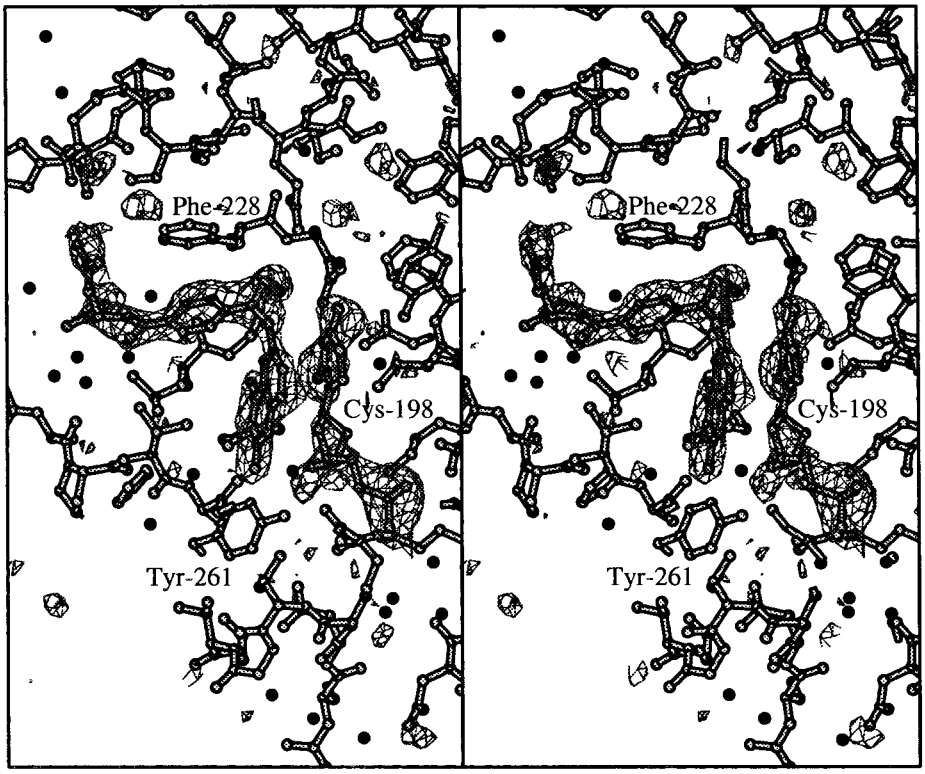

FIGURE 3: Section from an $(F_o - F_c)\alpha_{calc}$ omit map, where the α_{calc}'s were calculated from the D221(169)N TS−dUMP−CB3717 structure that had been refined by simulated annealing (starting temperature of 1500 K) (*20*) without ligands. The map is contoured at 2.5σ. Superimposed on the map is a MOLSCRIPT (*34*) plot of the structure, with the ligands in dark gray, the protein in gray, and ordered water as black spheres.

oxygen in the carboxamide group points into the protein where it hydrogen bonds to another ordered water as in the wild-type structure; hydrogen bonding to this ordered water is unaffected by the substitution. Thus, we conclude the substituted Nδ2 of N221(169) in the mutant structure points into the active site, where it interacts with the cofactor.

The distance between N3 of CB3717 and Nδ2 of Asn-221(169) is 2.8 Å, and the side chain of Asn-221(169) is ideally oriented to form a hydrogen bond to N3 of CB3717. N3 of CB3717 cannot be protonated, since this would imply an unfavorable close contact with the hydrogens of Nδ2; therefore, CB3717 is most likely bound as the less-favored enol tautomer shown in Figure 5a. Consistent with this interpretation, the distance between the amide of Gly-225-(173) and OA4 of CB3717 increases in both crystallographically independent active sites, from a distance of 3.0 Å in wild-type TS to 3.1 Å, as would be expected if OA4 changed from a carbonyl to a hydroxyl group.

Mutation of Asp-221 results in other changes in hydrogen bonding which may contribute to the decreased stability of the D221(169)N ternary complex. A negative density peak at the site of Wat3 in the direct difference map indicates decreased occupancy or greater mobility of this water. In addition to moving outside hydrogen bonding distance from CB3717, it has also shifted away from the adjacent ordered water, so it only forms two hydrogen bonds in the mutant complex, compared to four in the wild-type complex. Wat2 is also shifted such that it no longer hydrogen bonds to the C terminus of the protein. In total, there are one less hydrogen bond to CB3717, three less hydrogen bonds to conserved waters Wat2 and Wat3, and one less hydrogen bond to the C terminus in the mutant than in the wild-type complex.

In the FdUMP−CH_2H_4folate Complex Structure, the Open Conformation of the Cofactor Is Disfavored or Is Prevented from Forming. Apo-TS or TS bound to dUMP alone crystallizes with an open conformation in the cubic space group $I2_13$ (*21*, *25*). Binding of cofactor or cofactor analogues to the enzyme, either in the presence or in the absence of substrate, normally induces the protein to undergo a conformational change which closes down the active site cavity and draws the C terminus toward the ligand binding sites. We have crystallized "closed" *E. coli* TS in hexagonal space group $P6_3$, with a dimer in the asymmetric unit, or in the trigonal space group $P3_121$, with a monomer in the asymmetric unit (*8*, *26*). Numerous crystallization trials with D221(169)N TS, FdUMP, and CH_2H_4folate, under conditions that are normally used to crystallize the ternary complex, yielded only cubic crystals, suggesting that the conformation change had not been induced in the protein. Formation of a covalent ternary complex with FdUMP and the cofactor in solution was monitored by SDS−PAGE (*7*). No band for TS covalently bound to FdUMP and CH_2H_4folate was observed after incubation of D221(169)N with FdUMP and CH_2H_4folate for 2 h. Similarly, no ternary complex formation was observed for *L. casei* D221N by Chiericatti and Santi (*7*). Ordinarily, we would have presumed that the cofactor had not been incorporated into the crystals. However, when we determined the crystal structure of these cubic crystals, we found two partially occupied binding sites for cofactor, even though the protein was clearly in the characteristic open conformation of the unliganded protein.

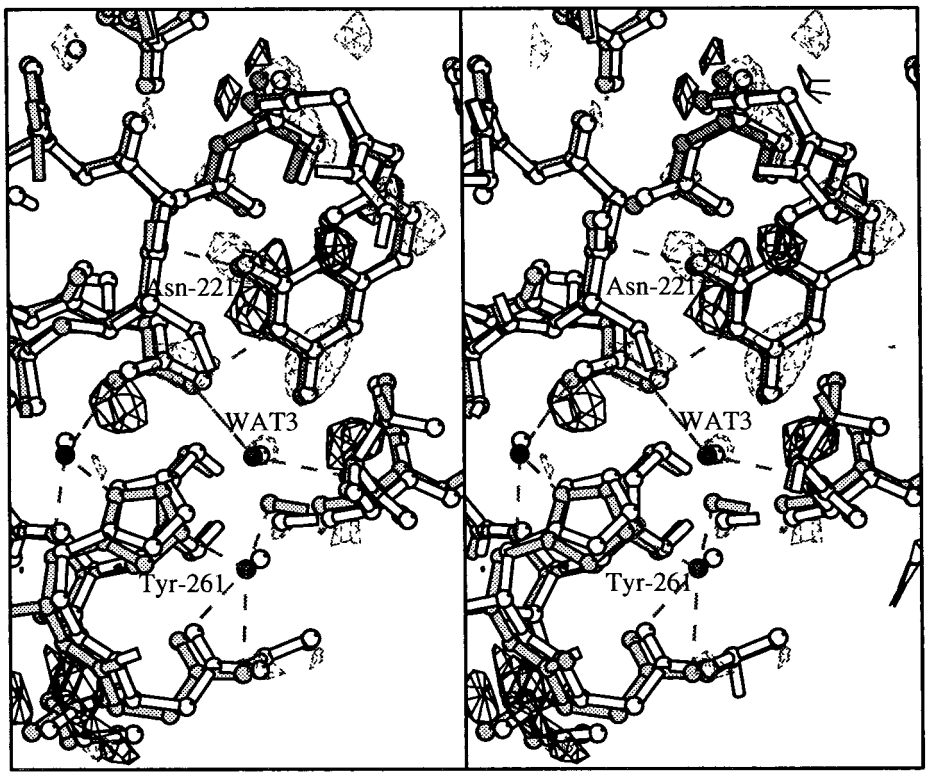

FIGURE 4: Section from an $(F_{o1} - F_{o2})\alpha_{calc}$ difference map, where F_{o1} and α_{calc} are an amplitude and phase, respectively, from D221(169)N TS−dUMP−CB3717 and F_{o2} is the corresponding amplitude from wild-type TS−dUMP−CB3717. The map is contoured at $+3\sigma$ with solid lines and -3σ with dashed lines. Superimposed on the map is a MOLSCRIPT (*34*) plot of wild-type TS−dUMP−CB3717 (in white) and D221(169)N TS−dUMP−CB3717. The color code for the D221(169)N TS structure is as follows: protein, light gray; ligands, dark gray; and waters, black spheres. Hydrogen bonds to water and CB3717 in the D221(169)N TS structure are drawn with dashed lines.

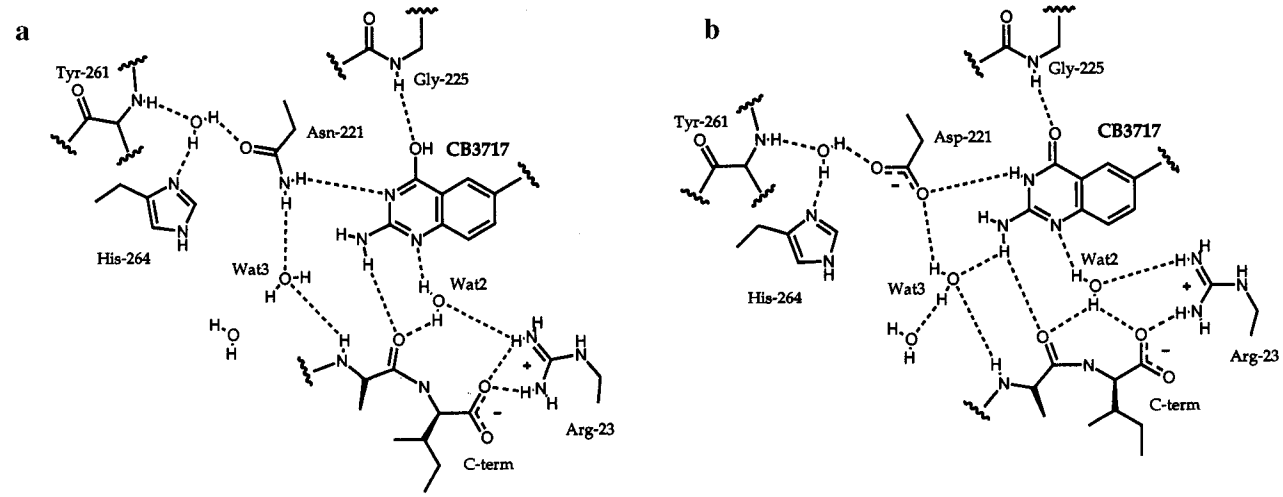

FIGURE 5: Schematic drawing of hydrogen bonds surrounding CB3717 in (a) D221(169)N TS−dUMP−CB3717 and (b) wild-type TS−dUMP−CB3717.

The most prominent density for the cofactor lay in a well-characterized, alternate nonproductive folate binding site that we have now identified in several crystal structures of *E. coli* and *L. casei* TS, including the binary complex of *E. coli* TS with the antifolate TS inhibitor CB3717 (*6*, *21*, *27*) (Figure 6). The CH_2H_4folate bound in the alternate site adopts an extended conformation, similar to that seen in solution (*28*), and does not interface with the pyrimidine ring of the substrate as seen in the productive mode. For this reason, we postulate that the alternate site may be an initial docking site, or a holding site for the cofactor prior to catalysis (*6*, *27*). In its productive binding site, corresponding to intermediate II (Figure 1), CH_2H_4folate adopts a folded conformation, in which the imidazolidine ring is open and the pterin ring makes approximately right angles to the PABA moiety, and stacks on top of the pyrimidine ring of the substrate (*8*, *11*).

Occupancy of the Novel Alternate Site Prevents Closure of the Active Site. The density for CH_2H_4folate in the "docking" site clearly shows that the cofactor has a closed five-membered imidazolidine ring (Figure 6) and that the conformation of the three-ring system is similar to the solution conformation of free CH_2H_4folate (*28*). The tetrahydropyrazine ring is in a half-chair conformation with

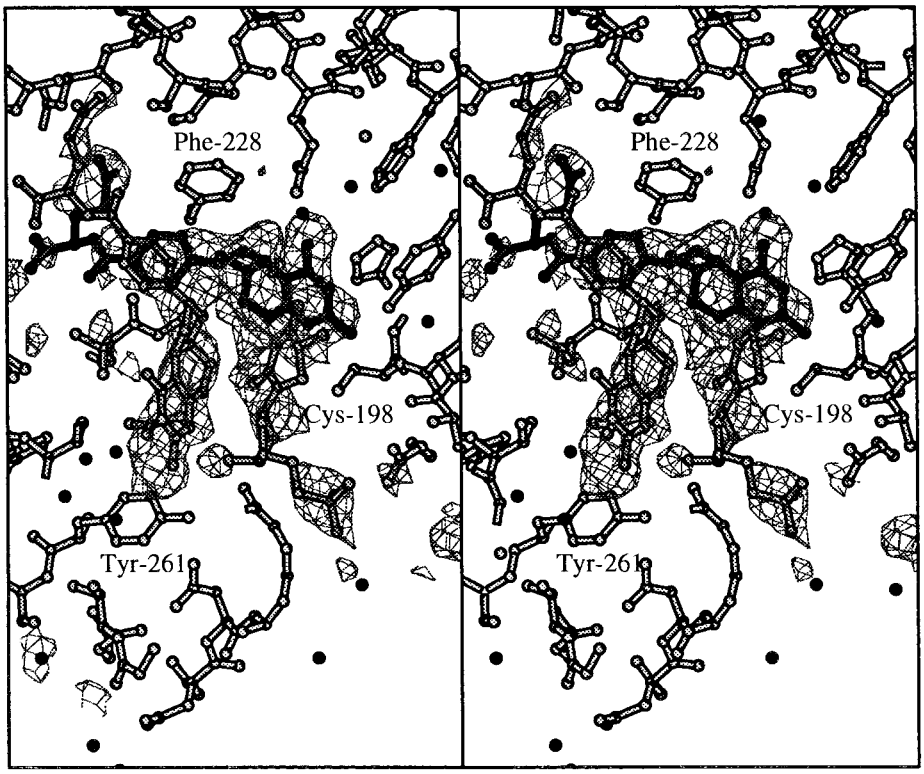

FIGURE 6: Section from an $(F_o - F_c)\alpha_{calc}$ omit map, where the α_{calc}'s were calculated from the D221(169)N TS−FdUMP−CH_2H_4folate structure that had been refined by simulated annealing (starting temperature of 1500 K) (*20*) without ligands. The map is contoured at 2.5σ. Superimposed on the map is a MOLSCRIPT (*34*) plot of the structure, with the ligands in dark gray, the protein in gray, and ordered water as black spheres.

the C6 hydrogen axial, and C6 on the opposite side of the ring plane with respect to C7. The imidazolidine ring appears to have an envelope conformation, with the PABA substituent equatorial, extending away from the pterin ring system. The PABA-Glu substituent was disordered (Figure 6), and the monoglutamyl tail could not be fitted to continuous density. Hydrogen bonds to the pterin ring could be only tentatively assigned since the elevated *B*-factors for the ligand increased the error in distances to neighboring atoms (Figure 7a). A hydrogen bond between Tyr-146(94) and N3 of the pterin ring is conserved in other structures of folates in this binding site (*6*, *27*). A hydrogen bond between His-199(146) Nϵ2 and the carbonyl substituent of the pterin ring (OA4) is also observed in the complex of *L. casei* TS with dUMP and CH_2H_4folate in the docking binding site (*27*).

Density for a second, nonproductive CH_2H_4folate binding site could be clearly distinguished in the unbiased difference map calculated after refinement of the protein with dUMP and CH_2H_4folate only in the initial docking site (Figure 8). In this second site, CH_2H_4folate has a closed imidazolidine ring, with the C6 hydrogen axial, and the PABA group extending away from the pterin ring. The imidazolidine ring has an envelope conformation, but with the flap, N10, on the side of the pterin ring opposite that in the first binding site. The pterin ring is bound "backward" in the active site cavity, rotated approximately 115° from its position in the productive ternary complex, such that mutant Asn-221(169) Nδ2 hydrogen bonds to the unprotonated N1 atom of the cofactor, instead of to the protonated N3 atom (Figures 7b and 8). In this new site, the pterin ring makes hydrophobic contacts with Leu-224(172) and Gly-225(173), and it effectively blocks movement of the C terminus into the active site to form the closed conformation of the protein, necessary for productive catalysis (Figures 7b and 8). The PABA ring overlaps the PABA ring in the first binding site as determined from the fully occupied PABA density in the $2F_o - F_c$ map, and the correspondingly featureless remaining PABA density in the difference map (Figure 8).

Difference maps indicated that when optimally fitted to density, FdUMP would impinge on the first cofactor binding site. Thus, the crystal structure was refined as a statistical average of two TS complexes: one binary complex with CH_2H_4folate alone bound in the docking site of TS and a ternary complex with CH_2H_4folate bound in the second, novel, site, with FdUMP bound as in the wild-type enzyme. In simulated annealing omit maps, the density for C5, C6, and F of FdUMP was weak (Figure 6), suggesting that the FdUMP was an equilibrium mixture of covalently bound and noncovalently bound species, as has been observed in several other ternary complex structures (*24*). However, a covalent bond between Cys-198(146) Sγ and C6 of the FdUMP was imposed during refinement since this constraint lowered the free *R*-factor (*29*) by 0.1%.

During the final round of refinement, the occupancies of the ligands were refined (Table 1). The refined occupancy of FdUMP was 0.58, and the occupancy of CH_2H_4folate in the first (docking) site was 0.43, consistent with the assumption that these two sites were not both occupied in one protomer at the same time. The occupancy of CH_2H_4folate in the second, also nonproductive but new site was 0.35; thus, some TS in the crystal either contained only FdUMP or contained the cofactor in other, undetected binding modes. The space group of the crystal structure, $I2_13$, contained one protomer of the TS dimer in the asymmetric unit. The two

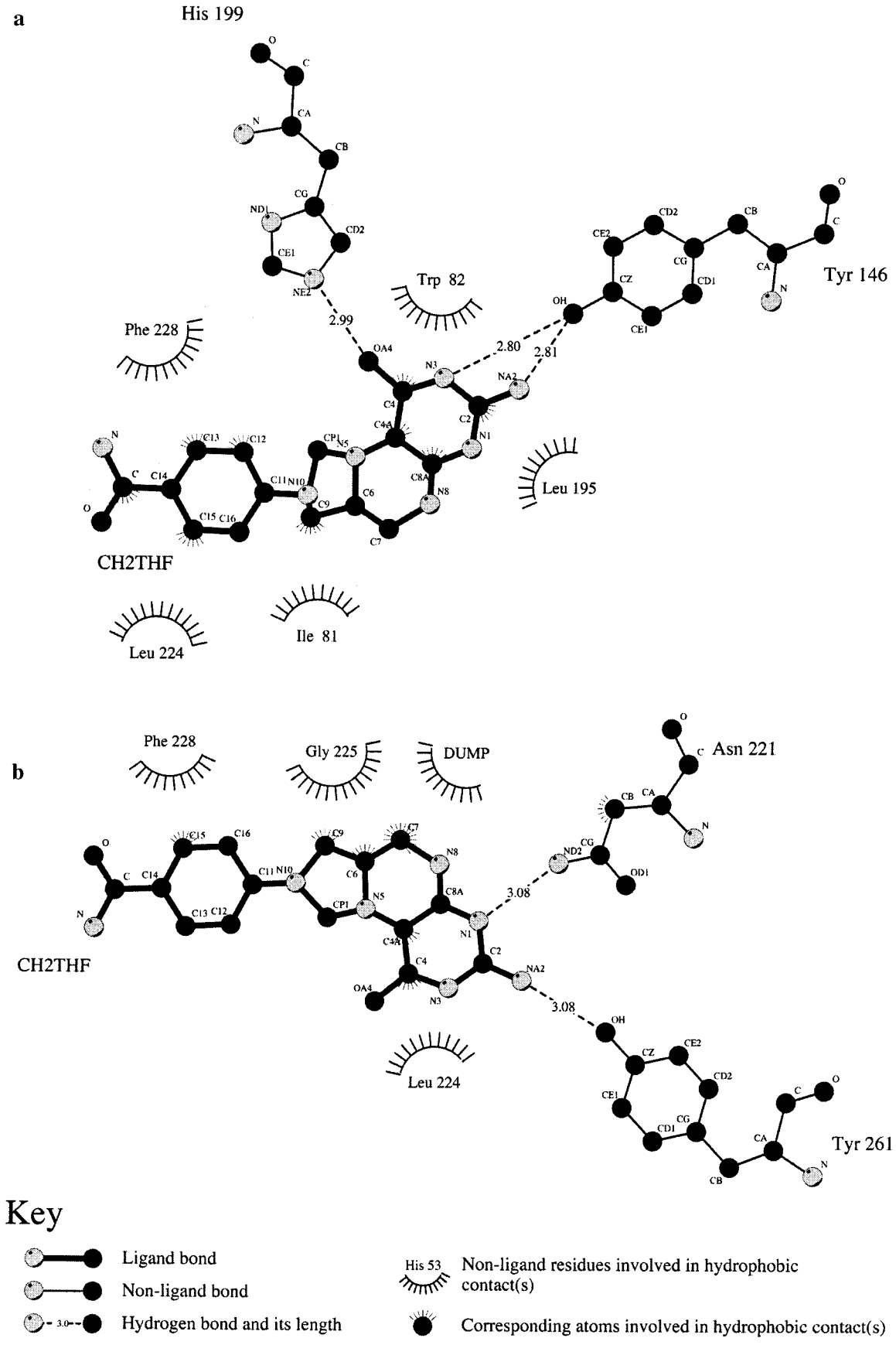

FIGURE 7: LIGPLOT (*35*) drawings of CH_2H_4folate−protein contacts for (a) the docking CH_2H_4folate binding site in D221(169)N TS−FdUMP−CH_2H_4folate and (b) the novel, nonproductive binding site.

protomers were therefore statistically identical, averaged by crystallographic symmetry. The individual molecules of TS may have CH_2H_4folate bound asymmetrically to the two active sites. Thus, one of these sites corresponds to the

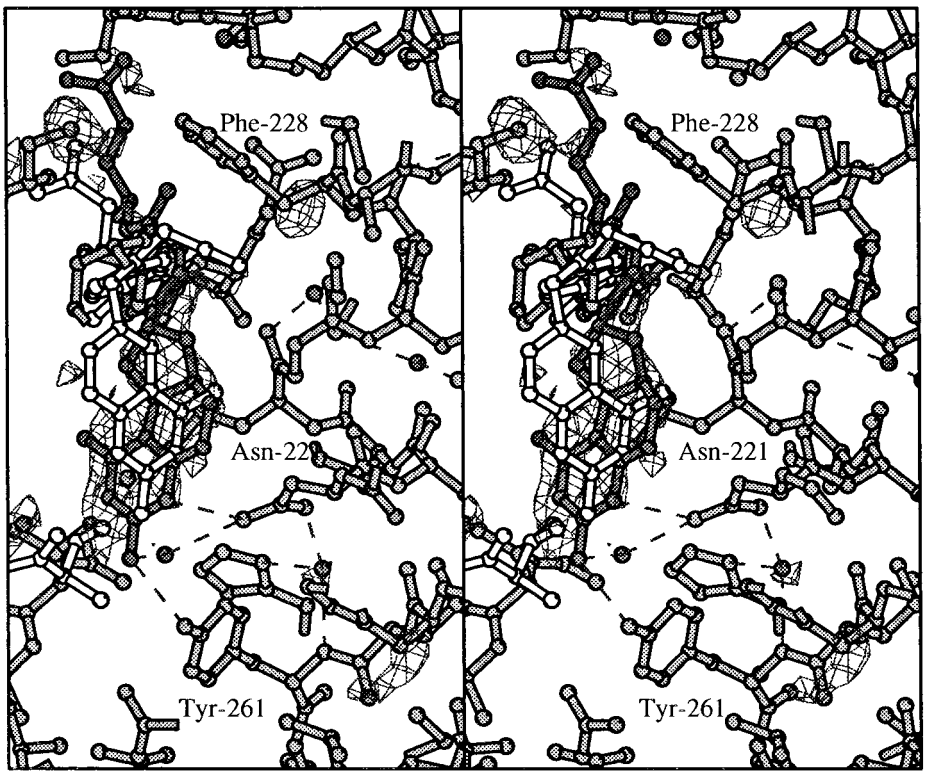

FIGURE 8: Section from an $(F_o - F_c)\alpha_{calc}$ map, where the α_{calc}'s were calculated from a refined D221(169)N TS−FdUMP−CH_2H_4folate structure that included CH_2H_4folate only in the first, docking site. Superimposed on the map is a MOLSCRIPT (*34*) plot of the structure, with the ligands and ordered water in black and the protein in gray. Also plotted in white, for comparison, are the C terminus and CB3717 from wild-type TS−dUMP−CB3717. Hydrogen bonds to ordered water and CH_2H_4folate are depicted with dashed lines.

previously observed initial docking site, and the other is brought about only by the mutation D221(169)N.

DISCUSSION

The structure of D221(169)N TS bound to dUMP and the folate analogue CB3717 is essentially identical to the wild-type complex (within 0.5 Å). This implies that, in its ring-opened form, the TS cofactor, CH_2H_4folate, can bind to D221(169)N in the productive orientation for formation of intermediate II (Figure 1). The elevated *B*-factors for the ligands in this structure suggest that the complex is less stable than that formed by the wild-type enzyme. Furthermore, D221(169)N TS is clearly in the closed conformation seen in wild-type ternary complexes, and dUMP is covalently attached to Cys-198, as in the wild type. This result implies that the inability of D221(169)N to form detectable amounts of the TS−FdUMP−CH_2H_4folate covalent complex is the result of impairment of early steps in cofactor binding: ring opening and alignment with the substrate.

The mechanism of cofactor binding is not completely understood. The kinetic mechanism of the TS reaction is generally acknowledged to be ordered and sequential, with dUMP binding first, except when the reaction occurs in phosphate buffer (*3*, *30*). The crystal structures of ternary complexes show clearly that to form the covalent intermediate II, dUMP must be bound first, providing a binding surface for the pterin ring of cofactor (*8*, *11*). Binary complexes of TS and cofactor have been detected by equilibrium dialysis, but the cofactor is much more weakly bound to the enzyme than in the presence of dUMP (*31*). The cofactor is believed to bind to TS in a two-step process: first, formation of a rapidly reversible, weakly bound ternary complex; and second, conversion of the noncovalent complex to a tight, reversible, covalent complex (*30*, *32*). During these binding steps, the five-membered imidazolidine ring of the cofactor opens, producing a reactive iminium ion which adds to C5 of dUMP (*32*). The initial binding site on TS for CH_2H_4-folate is not known, but must be different from the binding site seen in crystal structures of analogues of intermediate II (e.g., Figure 3), where CH_2H_4folate is in a conformation incompatible with a closed imidazolidine ring (*8*, *10*, *11*). It is also not known at what point, or by what mechanism, the cofactor is converted to its reactive iminium ion form. Several investigators have proposed that the TS conformational change drives ring opening (*24*, *30*, *32*), possibly by promoting the planar, quinoid form of the PABA-Glu moiety seen by Raman spectroscopy (*33*). Also unclear is the basis for asymmetric binding affinities for antifolates and CH_2H_4-folate binding to the two active sites of the homodimer (*31*).

Against this backdrop of information about cofactor binding, there are a number of possible interpretations of the structure of the D221(169)N TS ternary complex with FdUMP and CH_2H_4folate. The structure reveals two independent, ~50% occupied binding sites for CH_2H_4folate, and shows FdUMP bound with ~50% occupancy to the productive binding site for dUMP. The FdUMP binding site is compatible with only one of the cofactor binding sites, and would run into severe steric clash with the other. Thus, in a portion of the TS protomers, CH_2H_4folate is bound as a binary complex. Since this complex was crystallized from the phosphate buffer where binding of the substrate and cofactor is randomly ordered, occupancy of the docking site may be enhanced to the point where an asymmetric complex is obtained. It may be that occupancy of the two CH_2H_4-

folate sites is random. Alternatively, each TS molecule may form a nonproductive ternary complex in one active site, and a cofactor binary complex at the other. This kind of asymmetry is consistent with the half of the sites reactivity of TS. These two alternatives cannot be distinguished from the crystal structure, since any nonequivalence of the two protomers in the TS homodimer is averaged throughout the crystalline lattice by crystallographic symmetry.

The highest-occupancy cofactor binding site is equivalent to the binding site for CB3717 in the *E. coli* TS−CB3717 binary complex (*21*) and to the CH_2H_4folate binding site in crystals of *L. casei* TS−dUMP soaked in cofactor (*27*). CB3717 also binds at this site in one protomer of *E. coli* TS E60(58)Q−dUMP−CB3717 (*6*). The fact that the cofactor in this alternate site clearly has a closed five-membered ring and a conformation resembling CH_2H_4folate in solution (*28*) suggests that this alternate site may be the docking site for cofactor in a two-step mechanism for binding of CH_2H_4folate (*30*). However, it may instead be a nonproductive binding site that is off the TS reaction path. The second, lower-occupancy cofactor binding site in the D221(169)N TS structure is almost certainly a nonproductive binding mode unique to the D221(169)N mutant, since the carboxyl of D221(169) in the wild-type enzyme would not hydrogen bond to N1 of CH_2H_4folate, both being hydrogen bond acceptors in the mutant (Figure 7b).

Given the possible interpretations of the D221(169)N TS−FdUMP−CH_2H_4folate structure, there are at least four possible explanations for the inactivity of this TS. First, the cofactor may bind only to nonproductive, off-pathway binding sites in D221(169)N TS. Second, the cofactor may bind at a nonproductive site in one of the protomers that blocks the enzyme conformational change required to form the productive ternary complex in the other active site. Third, the cofactor may bind a portion of the time to its initial on-pathway binding site in the mutant, but the mutation has shifted the equilibrium between open and closed forms of CH_2H_4folate toward the closed ring form so that a tight covalent complex never forms. Fourth, D221(169) may be essential to a chemical step that opens the imidazolidine ring. Evidence that does not support the latter possibility is the ability of D221A in *L. casei* TS to form a covalent ternary complex with FdUMP and CH_2H_4folate (*7*).

These mechanisms for inactivation of TS by mutating D221(169) to Asn are not mutually exclusive, and all may be involved to some extent. Asp-221 may have a direct role in conversion of the cofactor to its reactive, ring-open form, and certainly provides important ligand interactions which stabilize the covalent ternary complex. A further role for Asp-221, which helps explain its absolute conservation across TS species, may be to exclude nonspecific binding modes of CH_2H_4folate in the spacious enzyme active site. We are determining structures of other D221 mutant complexes to further define the role of Asp-221 in the TS reaction.

REFERENCES

1. Climie, S., Ruiz-Perez, L., Gonzalez-Pacanowska, D., Prapunwattana, P., Cho, S. W., Stroud, R., and Santi, D. V. (1990) *J. Biol. Chem. 265* (31), 18776−9.
2. Michaels, M. L., Kim, C. W., Matthews, D. A., and Miller, J. H. (1990) *Proc. Natl. Acad. Sci. U.S.A. 87* (10), 3957−61.
3. Carreras, C. W., and Santi, D. V. (1995) *Annu. Rev. Biochem. 64*, 721−62.
4. Huang, W., and Santi, D. V. (1994) *J. Biol. Chem. 269* (50), 31327−9.
5. Hardy, L. W., Graves, K. L., and Nalivaika, E. (1995) *Biochemistry 34*, 8422−32.
6. Sage, C. R., Rutenber, E. E., Stout, T. J., and Stroud, R. M. (1996) *Biochemistry 35*, 16270−81.
7. Chiericatti, G., and Santi, D. V. (1998) *Biochemistry 37*, 9038−42.
8. Montfort, W. R., Perry, K. M., Fauman, E. B., Finer-Moore, J. S., Maley, G. F., Hardy, L., Maley, F., and Stroud, R. M. (1990) *Biochemistry 29* (30), 6964−77.
9. Finer-Moore, J. S., Montfort, W. R., and Stroud, R. M. (1990) *Biochemistry 29* (30), 6977−86.
10. Matthews, D. A., Villafranca, J. E., Janson, C. A., Smith, W. W., Welsh, K., and Freer, S. (1990) *J. Mol. Biol. 214* (4), 937−48.
11. Matthews, D. A., Appelt, K., Oatley, S. J., and Xuong, N. H. (1990) *J. Mol. Biol. 214* (4), 923−36.
12. Kunkel, T. A., Roberts, J. D., and Zakour, R. A. (1987) *Methods Enzymol. 154*, 367−82.
13. Belfort, M., Maley, G., Pedersen-Lane, J., and Maley, F. (1983) *Proc. Natl. Acad. Sci. U.S.A. 80* (16), 4914−8.
14. Climie, S. C., Carreras, C. W., and Santi, D. V. (1992) *Biochemistry 31*, 6032−8.
15. Maley, G. F., and Maley, F. (1988) *J. Biol. Chem. 263* (16), 7620−7.
16. Wahba, A. L., and Friedkin, M. (1961) *J. Biol. Chem. 263* (2), PC11−2.
17. Otwinowski, Z. (1993) in *Proceedings of the CCP4 Study Weekend* (Sawyer, L., Isaacs, N., and Bailey, S., Eds.) pp 56−62, SERC Daresbury Laboratory, Warrington, U.K.
18. Chambers, J. L., and Stroud, R. M. (1977) *Acta Crystallogr., Sect. B 33*, 1824−37.
19. Brunger, A. T. (1992) *X-PLOR Version 3.1. A System for X-ray Crystallography and NMR*, Yale University Press, New Haven, CT.
20. Brunger, A. T. (1988) *J. Mol. Biol. 203* (3), 803−16.
21. Stout, T. J., Sage, C. R., and Stroud, R. M. (1998) *Structure 6*, 839−48.
22. Santi, D. V., McHenry, C. S., and Sommer, H. (1974) *Biochemistry 13*, 471−81.
23. Jones, T. R., Calvert, A. H., Jackman, A. L., Brown, S. J., Jones, M., and Harrap, K. R. (1981) *Eur. J. Cancer 17*, 11−9.
24. Hyatt, D. C., Maley, F., and Montfort, W. R. (1997) *Biochemistry 36*, 4585−94.
25. Perry, K. M., Fauman, E. B., Finer-Moore, J. S., Montfort, W. R., Maley, G. F., Maley, F., and Stroud, R. M. (1990) *Proteins 8* (4), 315−33.
26. Fauman, E. B., Rutenber, E. E., Maley, G. F., Maley, F., and Stroud, R. M. (1994) *Biochemistry 33* (6), 1502−11.
27. Birdsall, D. L., Finer-Moore, J., and Stroud, R. M. (1996) *J. Mol. Biol. 255*, 522−35.
28. Poe, M., Jackman, L. M., and Benkovic, S. J. (1979) *Biochemistry 18*, 5527−30.
29. Brunger, A. T. (1992) *Acta Crystallogr., Sect. D 49*, 24−36.
30. Spencer, H. T., Villafranca, J. E., and Appleman, J. R. (1997) *Biochemistry 36*, 4212−22.
31. Dev, I. K., Dallas, W. S., Ferone, R., Hanlon, M., McKee, D. D., and Yates, B. B. (1994) *J. Biol. Chem. 269*, 1873−82.
32. Santi, D. V., McHenry, C. S., Raines, R. T., and Ivanetich, K. M. (1987) *Biochemistry 26*, 8606−13.
33. Austin, J. C., Fitzhugh, A., Villafranca, J. E., and Spiro, T. G. (1995) *Biochemistry 34* (23), 7678−85.
34. Kraulis, P. J. (1991) *J. Appl. Crystallogr. 24*, 946−50.
35. Wallace, A. C., Laskowski, R. A., and Thornton, J. M. (1995) *Protein Eng. 8*, 127−34.

BI9810510